

# Robustness Experiments for a Planar Hopping Control System

**Kale Harbick and Gaurav S. Sukhatme**

*kale|gaurav@robotics.usc.edu*

Robotic Embedded Systems Laboratory

Robotics Research Laboratory

Department of Computer Science

University of Southern California

Los Angeles, CA 90089-0781

## ABSTRACT

We explore the robustness of a control system for a pneumatic monopod simulation by adding Gaussian noise to the sensors and actuators. The control system is based on Raibert's three-part control system decomposition; with significant modifications to two of the control loops. Our speed controller uses a neural network to approximate the neutral point function, and we use a model-based height controller. No changes were made to the attitude controller. Simulation experiments show that the control system performs stably in the noisiest case, with a relative error of approximately 20%. The control system is expected to perform comparably on the real robot since our actual sensors are more accurate compared to the sensors simulated in these experiments.

## 1 INTRODUCTION

The benefits of legged systems over other forms of terrestrial locomotion are obvious; they can navigate obstacles which wheeled and treaded vehicles cannot. Dynamically-stable legged systems have advantages over statically-stable legged systems. Running machines can travel faster and can navigate terrain which has points of support that are spaced too far apart for walking machines to reach. Even for the simplest running machine, a one-legged hopper, several research problems have not been completely solved.

Most running machines constructed thus far have served as little more than existence proofs of different forms of locomotion. We seek to construct a running machine that builds on basic locomotion with additional behaviors that would be useful in a more functional robotic system. To this end we have studied ways to improve the traditional Raibert three-part control system [1].

The hopping machine considered in this paper is like a pogo-stick, except it uses a pneumatic rather than mechanical spring. To simplify the analysis, we restrict the motion of the robot hopper to the sagittal plane. A diagram of the hopper model is shown in Figure 1. Table 1 defines the subscripts used in the equations, Table 2 defines the state variables, and Table 3 defines the physical parameters of the hopper. The leg stroke, hip offset, and mass parameters are similar to those of the planar hopping machine reported in [1].

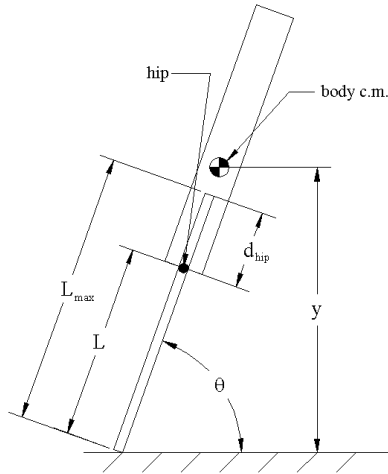


*Figure 1: 2D hopping machine in stance. The body is not shown.*

Our controller is based on Raibert's three-part control system [1]. This method decomposes the control into three separate control loops: forward velocity control, body attitude control, and height control. The experiments reported in this paper use a model-based height controller [2], and a speed controller which uses a simple neural network to approximate the neutral point function [3]. The body attitude controller is unchanged from Raibert's original design.

Simulation experiments were performed first with no noise and then with several combinations of two sources of sensor noise and one source of actuator noise. All the noise sources were modeled as zero-mean, Gaussian, with no correlation across sources.

The noisiest case tested, gave a relative error of approximately twice that of the noiseless case. The simulated sensors with the least noise are of lower accuracy than the actual sensors we plan to use for the real robot.

The paper is organized as follows. Related work is discussed in Section 2. Section 3 summarizes the control system. Experimental results are presented in Section 4. Conclusions and future work are discussed in Section 5.

## 2 RELATED WORK

A three-part control system has been used to control monopod hopping robots [1]. This system used a fixed duration thrust to regulate hopping height, and two PD-controllers to regulate forward running speed.

Proportional control has been used to regulate hopping height in simulation [4]. For the Monopod II robot, an adaptive energy feedback controller was used to control the apex energy and thus the apex height [5]. A similar approach to Raibert's for controlling running speed modifies the neutral point approximation with an additional factor of the ratio of leg length to rest length [4].

A discrete closed form trajectory model was used to control a bow leg hopper [6]. Model pa-

|      |                    |
|------|--------------------|
| $td$ | touch-down         |
| $lo$ | lift-off           |
| $+$  | immediately after  |
| $-$  | immediately before |
| $d$  | desired value      |

**Table 1:** Subscript definitions.

|                |  |
|----------------|--|
| $L$            | leg length ( $m$ )   |
| $y$            | height of body c.m. ( $m$ )  |
| $\dot{y}$      | body vertical velocity ( $m/s$ )                                       |
| $\dot{x}$      | body horizontal velocity ( $m/s$ )                                     |
| $K_s$          | spring constant ( $N \cdot m$ )  |
| $\theta$       | angle of leg measured from ground ( $rad$ )                            |
| $\dot{\theta}$ | angular velocity of leg ( $rad/s$ )                                    |
| $I$            | moment of inertia of body w.r.t. foot during stance ( $kg \cdot m^2$ ) |
| $x_f$          | distance from body c.m. to foot along horizontal dimension ( $m$ )     |
| $T_s$          | stance duration ( $s$ )  |
| $\phi$         | body angle w.r.t. horizontal ( $rad$ )                                 |
| $\gamma$       | angle of leg w.r.t. body ( $rad$ )                                     |

**Table 2:** Variable definitions.

parameters were experimentally determined with a least squares fit to a set of recorded trajectories.

A simulation of a vertical hopping machine was controlled using a near-inverse discrete-time model [7]. Time-varying or unknown parameters were estimated with a recursive least-squares parameter estimator. Because the model was able to update itself in this way, the controller was much less sensitive to modeling errors and even abrupt changes in physical parameters.

Other statistical learning methods such as RMRC have been used to learn inverse kinematic mappings in real time [8].

Our speed controller approximates the neutral point function using a simple neural network, rather than a linear function of forward velocity and stance duration. This allows the controller to track desired speeds beyond the point at which Raibert’s approximation diverges from linear. For the plant simulated in these experiments, this point is approximately  $0.7 m/s$ .

### 3 CONTROL SYSTEM

#### 3.1 Height Control

The height control loop functions as follows. At lift-off, the controller solves equations of motion for the next five phases: initial ascent, descent, compression, extension, and final ascent. The goal is to control the apex height  $y_{max}^{k+1}$  reached at the end of the final ascent phase. The controller uses state information at the beginning of initial ascent (lift-off) and the goal apex height to calculate the proper leg length setting. As the hopper transitions from initial ascent to descent, the leg setting is realized with a PD controller

|           |                                       |                                   |
|-----------|---------------------------------------|-----------------------------------|
| $g$       | gravitational acceleration            | $-9.81 \text{ m/s}^2$             |
| $\mu_k$   | viscous leg friction                  | $5.0 \text{ N/s}$                 |
| $d_{hip}$ | distance from hip to body c.m.        | $0.05 \text{ m}$                  |
| $L_{max}$ | max leg length                        | $0.285 \text{ m}$                 |
| $m_s$     | sprung mass                           | $8.375 \text{ kg}$                |
| $m_u$     | unsprung mass                         | $0.225 \text{ kg}$                |
| $A_p$     | area of piston                        | $4.91 \times 10^{-4} \text{ m}^2$ |
| $P_0$     | nominal pressure of upper leg chamber | $4.0 \times 10^2 \text{ kPa}$     |

**Table 3:** Physical parameters of the hopper.

$$\tau = -K_P (L - L_d) - K_D \dot{L}$$

where  $\tau$  is the leg force command, and  $K_P$  and  $K_D$  are proportional and derivative gains. Values for  $K_P$  and  $K_D$  used in the simulations are  $1300.0 \text{ N/m}$  and  $50.0 \text{ N/(m/s)}$ , respectively.

This leg position is maintained until touch-down, at which point the actuator releases and the passive dynamics of stance take over. At lift-off the cycle begins again.

First we define the spring constant  $K_s$

$$K_s = A_p P_s L_{max}. \quad (1)$$

There are two equations of motion for compression and extension

$$\frac{dL}{d\dot{y}} = \frac{\dot{y}}{\left( \frac{K_s \sin \theta}{m_s L} - \frac{\mu_k \dot{y}}{m_s} + g \right) \sin \theta} \quad (2)$$

$$\frac{d\theta}{d\dot{y}} = \frac{\dot{\theta}_{lo}^{k+1} L_{max}^2}{\left( \frac{K_s \sin \theta}{m_s L} - \frac{\mu_k \dot{y}}{m_s} + g \right) L^2} \quad (3)$$

where

$$\dot{\theta}_{lo}^{k+1} = \frac{\dot{x}_{lo}^{k+1} \sin(\pi - \theta_{lo}^{k+1}) + \dot{y}_{lo}^{k+1} \cos(\pi - \theta_{lo}^{k+1})}{L_{max}}. \quad (4)$$

Equations 1 - 4 are the key equations for this model; see [9] and [2] for further details.

## 3.2 Speed Control

### 3.2.1 Raibert Controller

The neutral point of a hop is the point where the foot should be placed which will result in zero net acceleration [1]. This point is a function of hopping height and forward speed. Raibert used an approximation of the CG print, i.e. the locus of points on the ground over which the

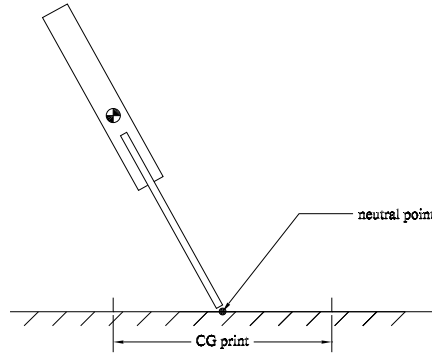


**Figure 2:** The neutral point is approximated using an estimation of the CG print.

body center of mass travels during stance, to estimate the neutral point. This is represented in Figure 2.

The length of the CG print was estimated as the stance duration times the forward running speed, as given below in Equation 5.

$$x_f = \frac{\dot{x}T_s}{2} + k_{\dot{x}}(\dot{x} - \dot{x}_d). \quad (5)$$

This foot position is converted into a desired leg angle w.r.t. the body

$$\gamma_d = \phi - \arcsin \frac{x_f}{L}.$$

Finally a second PD loop is used to calculate the hip torque

$$\tau = -k_p(\gamma - \gamma_d) - k_d(\dot{\gamma}).$$

We used the following values for gains:  $k_{\dot{x}} = 0.03$ ,  $k_p = 47.0$ ,  $k_d = 1.26$ .

### 3.2.2 Neural Network-Based Controller

One problem with the Raibert speed controller, as he points out, is that the neutral point is nearly linear with forward speed only up to a certain velocity. This point varies with the physical parameters of the system, but for the plant described in this paper, it is approximately  $0.7 \text{ m/s}$ . To overcome this difficulty, we used a simple neural network to more closely represent the neutral point function.

The original controller was modified to replace the first term in Equation 5 with a neural network output. The second term is left unchanged.

Training data were generated by a human operator controlling the foot position at varying speeds and apex heights. The simulation recorded neutral point values for two apex heights

| Noise Profile   | Avg. Rel. Error (%) |
|---|---------------------|
| No noise  | 11.6                |
| $\sigma_l = 1 \text{ cm}, \sigma_a = 1^\circ, \sigma_t = 5 \text{ N}\cdot\text{m}$  | 14.7                |
| $\sigma_l = 1 \text{ cm}, \sigma_a = 1^\circ, \sigma_t = 10 \text{ N}\cdot\text{m}$ | 16.9                |
| $\sigma_l = 1 \text{ cm}, \sigma_a = 2^\circ, \sigma_t = 5 \text{ N}\cdot\text{m}$  | 17.4                |
| $\sigma_l = 1 \text{ cm}, \sigma_a = 2^\circ, \sigma_t = 10 \text{ N}\cdot\text{m}$ | 16.1                |
| $\sigma_l = 2 \text{ cm}, \sigma_a = 1^\circ, \sigma_t = 5 \text{ N}\cdot\text{m}$  | 13.7                |
| $\sigma_l = 2 \text{ cm}, \sigma_a = 1^\circ, \sigma_t = 10 \text{ N}\cdot\text{m}$ | 14.9                |
| $\sigma_l = 2 \text{ cm}, \sigma_a = 2^\circ, \sigma_t = 5 \text{ N}\cdot\text{m}$  | 20.5                |
| $\sigma_l = 2 \text{ cm}, \sigma_a = 2^\circ, \sigma_t = 10 \text{ N}\cdot\text{m}$ | 18.6                |

**Table 4:** Average relative errors as percentages.

and five speeds, for a total of ten training points. The neural network was trained off-line using Levenberg-Marquardt optimization [10, 11].

## 4 EXPERIMENTS

In each run, the desired speed was varied from  $0.2 \text{ m/s}$  to  $1.8 \text{ m/s}$ , while the desired apex height remained constant. Three heights were tested, with eight different noise profiles (and one with no noise), for a total of 27 runs. The heights used were  $0.4 \text{ m}$ ,  $0.45 \text{ m}$ , and  $0.5 \text{ m}$ . These heights correspond to the planned operating range of our actual robot, which is being constructed. The length and angle measurements were contaminated with additive Gaussian noise, as were the torque settings. Two values for standard deviations were used for each noise source:  $1 \text{ cm}$  and  $2 \text{ cm}$  for leg length,  $1^\circ$  and  $2^\circ$  for angle, and  $5 \text{ N}\cdot\text{m}$  and  $10 \text{ N}\cdot\text{m}$  for hip torque. Note that the noise sources are uncorrelated with each other.

Height and speed tracking performances for no noise, minimum noise, and maximum noise are shown in Figure 3.

Table 4 shows the average relative error computed over all three heights for each noise profile.

Relative errors in forward velocity as functions of desired velocity and desired apex height are shown in Figure 4.

## 5 CONCLUSIONS AND FUTURE WORK

The experiments reported in this paper were intended to determine the sensitivity of the plant to additive Gaussian noise in what we presume to be the key actuator and sensors.

We found that the relative error of the test cases with the highest amounts of noise was approximately twice that of the noiseless case.

The leg length and angle sensors we plan to use on the physical robot have accuracies of  $2 \text{ mm}$  and  $0.7^\circ$ , respectively. The standard deviations for the noise of these sensors are  $0.67 \text{ mm}$  and  $0.23^\circ$ . Thus the noise for these sensors is less than the lowest noise case reported in these experiments. The noise profiles of our actuators have yet to be determined. However, the greatest

standard deviation for torque which was tested in these simulations ( $10 N \cdot m$ ) is approximately 25% of the maximum torque of the actuator. We believe that it is unlikely the true inaccuracy in torque will be greater than the values tested. We expect the controller will perform comparably on the real robot as it has in the simulations.

Future work in simulation includes 3D simulations and experiments with additional locomotory behaviors such as leaning against a wall and traversing inclined surfaces. We will also test the control system on a real hopping robot, which is being constructed.

## ACKNOWLEDGEMENTS

The authors would like to thank Michael Poole for his work on designing and constructing the physical robot frame, presently under development. The Vortex physics simulation toolkit developed by CM Labs was used for the experiments reported in this paper.

## REFERENCES

- [1] **Marc Raibert**, *Legged Robots that Balance*, MIT Press, Cambridge, MA, 1986.
- [2] **Kale Harbick and Gaurav S. Sukhatme**, “Controlling hopping height of a pneumatic monopod,” in *IEEE Intl. Conf. on Robotics and Automation*, 2002, vol. 4, pp. 3998–4003.
- [3] **Kale Harbick and Gaurav S. Sukhatme**, “Speed control of a pneumatic monopod using a neural network,” Tech. Rep. IRIS-02-413, Institute for Robotics and Intelligent Systems, University of Southern California, 2002.
- [4] **M. Ahmadi and M. Buehler**, “Stable control of a simulated one-legged running robot with hip and leg compliance,” *IEEE Transactions on Robotics and Automation*, vol. 13, no. 1, pp. 96–104, February 1997.
- [5] **M. Ahmadi and M. Buehler**, “The ARL Monopod II Running Robot: Control and Energetics,” in *IEEE Intl. Conf. on Robotics and Automation*, 1999, pp. 1689–1694.
- [6] **G.Z. Zeglin and H.B. Brown**, “Control of a bow leg hopping robot,” in *IEEE Intl. Conf. on Robotics and Automation*, 1998.
- [7] **Joseph Prosser and Moshe Kam**, “Control of hopping height for a one-legged hopping machine,” *Mobile Robots VII*, vol. 1831, pp. 604–612, November 1992.
- [8] **A. D’Souza and S. Vijayakumar and S. Schaal**, “Learning inverse kinematics,” in *IEEE Intl. Conf. on Intelligence in Robotics and Autonomous Systems*, 2001.
- [9] **Kale Harbick and Gaurav S. Sukhatme**, “Height control for a one-legged hopping robot using a two-dimensional model,” Tech. Rep. IRIS-01-406, Institute for Robotics and Intelligent Systems, University of Southern California, 2001.
- [10] **K. Levenberg**, “A method for the solution of certain non-linear problems in least squares,” *Quarterly Journal of Applied Mathematics*, vol. 2, no. 2, pp. 164–168, 1944.
- [11] **D. W. Marquardt**, “An algorithm for least-squares estimation of non-linear parameters,” *Journal of the Society of Industrial and Applied Mathematics*, vol. 11, no. 2, pp. 431–441, 1963.

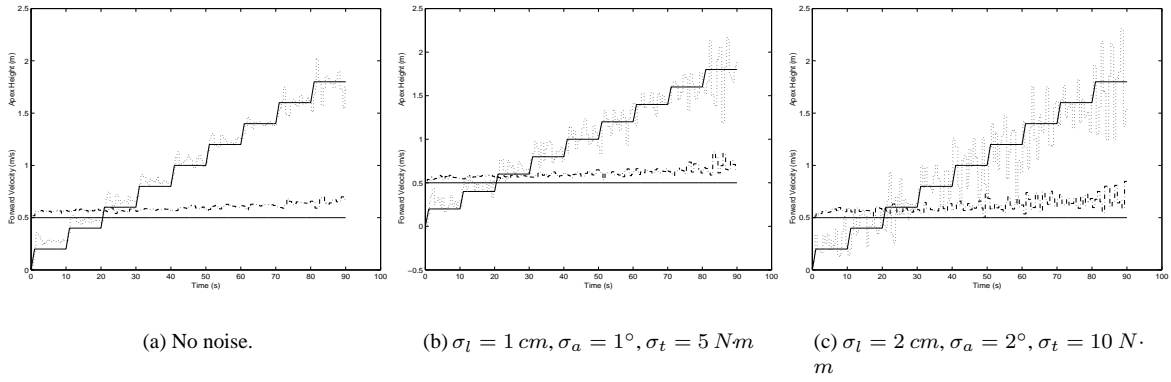


**Figure 3: Height and speed tracking.**

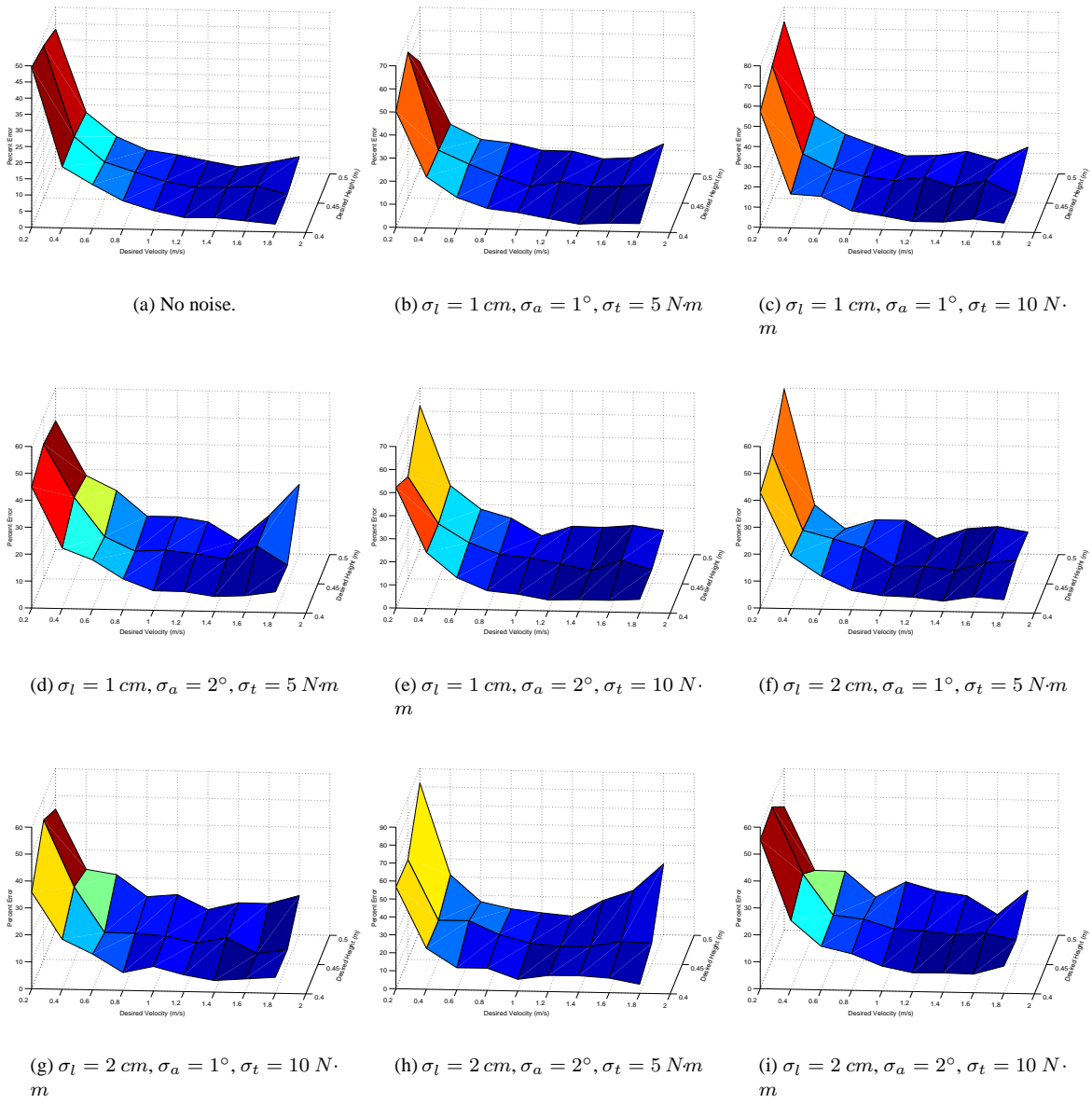


**Figure 4: Relative errors (in percentages) as a function of speed and height.**